Available online at www.sciencedirect.com
SCIENCE DIRECT
Journal of Chromatography B, 827 (2005) 109–118
JOURNAL OF CHROMATOGRAPHY B
www.elsevier.com/locate/chromb

LC–ESI-MS/MS determination of 4-hydroxy-*trans*-2-nonenal Michael adducts with cysteine and histidine-containing peptides as early markers of oxidative stress in excitable tissues

Marica Orioli, Giancarlo Aldini, Giangiacomo Beretta, Roberto Maffei Facino, Marina Carini *

Istituto Chimico Farmaceutico Tossicologico, Faculty of Pharmacy, University of Milan, Viale Abruzzi 42, 20131 Milan, Italy

Received 7 February 2005; accepted 27 April 2005
Available online 23 May 2005

Abstract

A sensitive, selective, specific and rapid liquid chromatographic–electrospray ionization tandem mass spectrometric assay was developed and validated for the simultaneous determination in skeletal muscle of the Michael adducts between 4-hydroxy-*trans*-2-nonenal (HNE), one of the most reactive lipid peroxidation-driven unsaturated aldehyde, and glutathione (GSH) and the endogenous histidine-containing dipeptides carnosine (CAR) and anserine (ANS), with the final aim to use conjugated adducts as specific and unequivocal markers of lipid peroxidation. Samples (skeletal muscle homogenates from male rats) were prepared by protein precipitation with 1 vol. of a $HClO_4$ solution (4.2%; w/v) containing H-Tyr-His-OH as internal standard. The supernatant, diluted (1:1, v/v) in mobile phase, was separated on a Phenomenex Sinergy polar-RP column with a mobile phase of water–acetonitrile–heptafluorobutyric acid (9:1:0.01, v/v/v) at a flow rate of 0.2 ml/min, with a run time of 12 min. Detection was on a triple quadrupole mass spectrometer equipped with an ESI interface operating in positive ionization mode. The acquisitions were in multiple reaction monitoring (MRM) mode using the following precursor → product ion combinations: H-Tyr-His-OH (IS): *m/z* 319.2 → 156.5 + 301.6; GS-HNE: *m/z* 464.3 → 179.1 + 308.0; CAR-HNE: *m/z* 383.1 → 110.1 + 266.6; ANS-HNE: *m/z* 397.2 → 109.1 + 126.1. The method was validated over the concentration ranges 1.5–90 (GS-HNE) and 0.4–40 (CAR-HNE, ANS-HNE) nmoles/g wet tissue, and the LLOQ were 1.25 and 0.33 pmoles injected respectively. The intra- and inter-day precisions (CV%) were <7.38% (≤10.90% at the LLOQs); intra- and inter-assay accuracy (RE%) was within ± 7.0% for all the concentrations (≤18% at the LLOQs). The method was applied to quantitate peptide-HNE Michael adducts in rat skeletal muscles exposed to oxidative stress to endogenously generate HNE, and the results indicate that CAR-HNE can be considered as an early, specific and stable marker of lipid peroxidation in excitable tissues.

Keywords: Glutathione; Histidine-containing peptides; Carnosine; Anserine; 4-Hydroxy-*trans*-2-nonenal; Michael adducts; LC–ESI-MS/MS; Oxidative stress markers; Rat skeletal muscle

1. Introduction

A number of age-related diseases have been shown to be associated with elevated levels of oxidatively modified proteins, and on the basis of various markers, their accumulation has been observed in cardiovascular diseases, atherosclerosis, long-term complications of diabetes, neurodegenerative diseases (Parkinson's disease, Alzheimer's disease). All amino acid residues of proteins are potential targets for oxidation by free radicals, leading to the formation of carbonyl derivatives [1]; alternatively carbonyl derivatives of proteins may be formed by interaction of protein amino acid side chains (mainly cysteine, histidine, and lysine residues) with reactive aldehydes, such as 4-hydroxy-*trans*-2-nonenal (HNE), acrolein (ACR) and malondialdehyde (MDA), generated by peroxidation of polyunsaturated fatty acids [2,3]. The facile reactivity of unsaturated aldehydes with thiols makes

* Corresponding author. Tel.: +39 02 50317532; fax: +39 02 50317565.
E-mail address: marina.carini@unimi.it (M. Carini).

1570-0232/$ – see front matter © 2005 Elsevier B.V. All rights reserved.
doi:10.1016/j.jchromb.2005.04.025

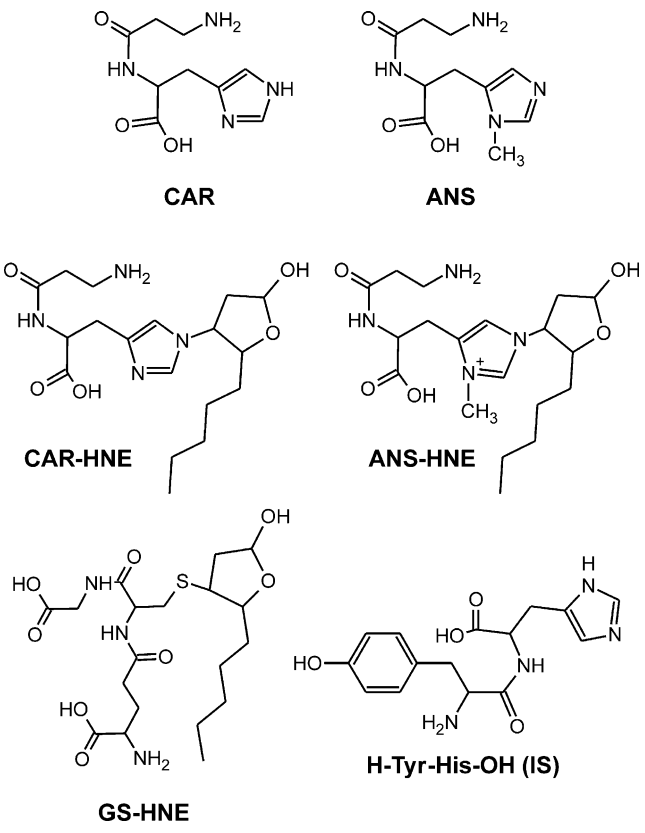

Fig. 1. Structures of HD peptides (CAR and ANS), H-Tyr-His-OH (IS) and of the carnosine, anserine and GSH Michael adducts with HNE (CAR-HNE, ANS-HNE, GS-HNE).

them ideal substrates for GSH, leading to the formation of thioether (Michael) adducts, that further undergo cyclization to form stable cyclic hemiacetals (Fig. 1). Hence conjugation with GSH to give Michael adducts, catalyzed by GSH-*S*-transferases, a well recognized pathway of detoxification of reactive aldehydes in living cells, can be considered as a first line of endogenous defence to prevent protein carbonylation [4–6]. Recently we have demonstrated that also endogenous histidine-containing dipeptides (HD) (Fig. 1), widely distributed in vertebrate animal tissues (especially skeletal muscles, heart and the central nervous system) such as carnosine (CAR; β-alanyl-L-histidine), homocarnosine (HCAR; γ-aminobutyryl-L-histidine) and anserine (ANS; *N*-β-alanyl-3-methyl-L-histidine) react with cytotoxic aldehydes (HNE and ACR) through a mechanism that has been elucidated by MS and NMR characterization of the conjugated products [7–9]. The carbonyl quenching ability of CAR and ANS has been confirmed by LC–MS/MS analysis (ESI interface) in complex biological matrices, by detection of conjugated adducts in spontaneously oxidized rat skeletal muscle [7,8]. This indicates that histidine-containing dipeptides behave as detoxifying agents for cytotoxic aldehydes, by reacting with HNE in biological systems through a "sacrificial" mechanism that mimicks the preferred HNE addition sites in proteins. According to this view, peptide-HNE adducts can be considered as specific and unequivocal markers of lipid peroxidation in those biological districts where they are specifically located, at high concentrations, such as CAR in brain and muscle (skeletal and cardiac). Since no methods are available for their determination in biological matrices, the aim of this work was to develop and validate a LC–MS/MS method for determination in rat skeletal muscle of HNE conjugated adducts with GSH and HD.

2. Experimental

2.1. Chemicals and reagents

All chemicals and reagents were of analytical grade and purchased from Sigma-Fluka-Aldrich Chemical Co (Milan, Italy). HPLC-grade and analytical-grade organic solvents were also purchased from Sigma-Aldrich (Milan, Italy). HPLC-grade water was prepared with a Milli-Q water purification system. Carnosine (β-alanyl-L-histidine) and the internal standard (IS) H-Tyr-His-OH were a generous gift from Flamma S.p.A. (Chignolo d'Isola, Bergamo, Italy). Anserine (*N*-β-alanyl-3-methyl-L-histidine) and the protease inhibitor cocktail were purchased from Sigma (Milan, Italy); heptafluorobutyric acid (HFBA), thiobarbituric acid (TBA), butylhydroxytoluene (BHT) and *N*-ethylmaleimide (NEM) from Aldrich (Milan, Italy); 2,2′-azobis(2-amidinopropane) dihydrochloride (AAPH) from Wako (Società Italiana Chimici, Rome, Italy). HNE was prepared by acid hydrolysis (1 mM HCl for 1 h at room temperature) of 4-hydroxy-non-2-enal diethylacetal (HNE-DEA), synthesized as previously reported [10] and quantitated by UV spectroscopy (λ_{max} 224 nm; ε $13.75 \times 10^4\ cm^{-1}\ M^{-1}$).

2.2. Equipments

Analyses were performed using a ThermoFinnigan Surveyor LC system equipped with a quaternary pump, a Surveyor UV–VIS Diode Array programmable detector 6000 LP, a Surveyor autosampler, a vacuum degasser, and connected to a TSQ Quantum Triple Quadrupole Mass Spectrometer (ThermoFinnigan Italia, Milan, Italy). Chromatographic separations were done by reverse phase elution with a Phenomenex Sinergy polar-RP column (150 mm × 2 mm i.d.; particle size 4 μm) (Chemtek Analytica, Anzola Emilia, Italy) protected by a polar-RP guard column (4 mm × 2 mm i.d.; 4 μm) kept at 25 °C. The mass spectrometer was equipped with an electrospray interface (ESI), which was operated in positive-ion mode, and controlled by the Xcalibur software (version 1.4).

2.3. Preparation of peptides-HNE adducts

HNE (0.5 ml of a 2 mM solution in 10 mM phosphate buffer, pH 7.4) was separately mixed with an equal volume of CAR, ANS and GSH (20 mM in 10 mM phosphate buffer, pH 7.4) and each mixture was incubated for 24 h at 37 °C to

obtain CAR-HNE, ANS-HNE and GS-HNE. At the end of the incubation period, sample aliquots were directly analysed by HPLC for the determination of HNE consumption, as previously described [8]. The final amount of HNE-adducts were calculated by considering that CAR, ANS and GSH form a 1:1 molar ratio adduct with HNE [8,10] and by calculating the residual amount of HNE (0% for GSH; 0.9% for CAR; 8.3% for ANS).

2.4. Preparation of stock solutions, calibration standards and quality controls

Two fresh stock solutions of ≈1 μmole/ml GS-HNE, CAR-HNE, ANS-HNE prepared as above described, the internal standard (IS; 0.1 μmole/ml), and the stock solution of BHT (10%, w/v in ethanol) were stored at 4 °C for one week. One solution was used to spike the tissue homogenate for calibration samples and the other to prepare the quality control (QC) samples (tissue homogenate). Stock solutions were diluted further with PBS and the solutions of each analyte were mixed together to obtain working solutions. The 200 nmoles/ml working solutions were analyzed by LC–MS/MS to ensure that the concentrations of the original solutions were within the limits of the maximum established error (≤3%). Calibration samples were prepared by spiking tissue homogenate (1:3, w/v in PBS) with each working solution to provide the following final concentrations: 1.5, 3, 6, 12, 30, 60 and 90 nmoles/g wet tissue for GS-HNE and 0.4, 0.8, 2.0, 4.0, 8.0, 20 and 40 nmoles/g for CAR-HNE and ANS-HNE. QC samples at four concentrations (1.5, 6, 30 and 90 nmoles/g for GS-HNE and 0.4, 2.0, 8.0 and 40 nmoles/g for CAR-HNE and ANS-HNE) were prepared in the same way. Each calibration sample was processed as described below. IS was added at the concentration of 40 nmoles/g wet tissue. Each calibration and QC sample was processed as described in sample preparation.

2.5. Sample preparation

Male Wistar rats (Charles River, Calco, Italy; body weight 250 ± 25 g) were maintained in compliance with the policy on animal care expressed in the National Research Council guidelines (NRC 1985). Food laboratory chow and drinking water were available ad libitum. Animals, anaesthetized with intraperitoneal sodium pentobarbital (60 mg/kg), were killed by decapitation and skeletal muscles (*tibialis* and *vastus*) were isolated and homogenized, using an Ultra-Turrax T25 homogenizer, in cold 100 mM phosphate buffer, pH 7.4 (1:3, w/v, 35.6 ± 5.2 mg protein/ml), containing 0.1% BHT (w/v). Aliquots of 0.5 ml of the homogenate were spiked with IS (40 nmoles/g wet tissue), deproteinized by addition of 0.5 ml of perchloric acid solution (4.2%; w/v) and vortexed for 1 min. After 15 min at 4 °C, the samples were centrifuged at 21,000 × *g* for 10 min. The supernatant was diluted (1:1, v/v) with the mobile phase, filtered through 0.45-μm nylon filters (Millex HV, PVDF membrane, 13 mm, MILLIPORE, Vimodrone, Milan, Italy) and the filtrate transferred to the autosampler vial insert (10 μl samples injected). Protein determinations were performed by a modified Lowry method [11] using bovine serum albumin as a standard.

2.6. Chromatographic and mass spectrometric conditions

Separations were done by gradient elution from 100% water–acetonitrile–heptafluorobutyric acid (A) (9:1:0.01, v/v/v) to 80% acetonitrile (B) in 12 min at a flow rate of 0.2 ml/min (injection volume 10 μl); the composition of the eluent was then restored to 100% A within 1 min and the system was reequilibrated for 6 min. The samples rack was maintained at 4 °C. ESI interface parameters (positive-ion mode) were set as follows: middle position; capillary temperature 270 °C; spray voltage 4.0 kV. Nitrogen was used as nebulizing gas at the following pressure: sheath gas 30 psi; auxiliary gas 5 a.u. MS conditions and tuning were performed by mixing through a T-connection the water-diluted stock solutions of analytes (flow rate 10 μl/min), with the mobile phase maintained at a flow rate of 0.2 ml/min: the intensity of the $[M + H]^+$ ions were monitored and adjusted to the maximum by using the Quantum Tune Master® software. Quantitations were performed in multiple reaction monitoring (MRM) mode at 2.00 kV multiplier voltage, and the following MRM transitions of $[M + H]^+$ precurson ions → product ions were selected for each analyte and the relative collision energies optimized by the Quantum Tune Master® software:

m/z 319.2 → 156.5 + 301.6 (collision energy, 25 eV) H-Tyr-His-OH (IS);
m/z 464.3 → 179.1 + 308.0 (collision energy, 27 eV) GS-HNE;
m/z 383.1 → 110.1 + 266.6 (collision energy, 35 eV) CAR-HNE;
m/z 397.2 → 109.1 + 126.1 (collision energy, 40 eV) ANS-HNE.

The following MRM transitions of $[M + H]^+$ precurson ions → product ions relative to GSH, CAR and ANS were used to detect in muscle tissues the endogenous peptides: *m/z* 308.1 → 162.1 + 179.1 (collision energy, 27 eV) for GSH; *m/z* 227.1 → 110.1 + 156.6 (collision energy, 38 eV) for CAR; *m/z* 241.2 → 95.2 + 109.2 (collision energy, 45 eV) for ANS.

The parameters influencing these transitions were optimized as follows: argon gas pressure in the collision Q2: 1.5 mbar; peak full width at half maximum (FWMH): 0.70 *m/z* at Q1 and Q3; scan width for all MRM channels: 1 *m/z*; scan rate (dwell time): 0.2 s/scan.

2.7. Assay validation

Analytical method validation was performed on *vastus* muscle in accordance to the recommendations published

by the FDA [12] (available from URL: http://www.fda.gov/cder/guidance/4252fnl.htm).

Calibration standards were prepared and analyzed in duplicate in three independent runs. The calibration curves were constructed by weighted ($1/x^2$) least-square linear regression analysis of the peak area ratios of GS-HNE, CAR-HNE and ANS-HNE to the IS against nominal analyte concentration. The lower limit of quantitation (LLOQ) was determined as the lowest concentration with values for precision and accuracy within ± 20% and a signal-to-noise (*S*/*N*) ratio of the peak areas ≥10.

Intra- and inter-day precisions and accuracies of the method were determined by assaying five replicates of each of the QC samples (four levels in the low, intermediate and high concentration range) in three separate analytical runs. Precision and accuracy were determined by calculating the coefficient of variation (CV%) and the relative error (RE%).

The absolute recovery of the analytes after protein precipitation was determined by comparing the mass spectrometric response of deproteinized tissue standards to that of deproteinized tissue blanks spiked with a corresponding set of concentrations (containing 100% of the theoretical concentration) over the entire calibration range. The overall absolute recovery was measured as the ratio of the slopes of the two calibration curves, and expressed as percentage.

The specificity of the assay and matrix-to-matrix reproducibility were evaluated by comparison of LC–MS/MS chromatograms of analytes at the LLOQ to those of blank tissue samples in triplicate.

Stability test was performed using QCs at two concentration levels (30 and 90 nmoles/g for GS-HNE; 20 and 40 nmoles/g for CAR-HNE and ANS-HNE) for short-term stability (kept at 4 °C for 1 h), long-term stability (processed samples stored at −20 °C for 4 weeks), and for three freeze/thaw cycles. All determinations were carried out in triplicate. The stability of processed sample, including the resident time in the autosampler (24 h at 4 °C), and stock solutions stability (4 weeks at 4 °C) were also determined in triplicate. The mean values of the triplicate samples were compared to the initial condition for all the stability tests.

2.8. Michael adducts formation in HNE-supplemented and peroxidized rat skeletal muscles

Two millilitres of aliquots of the *vastus* and *tibialis* homogenates prepared without BHT (35.6 ± 5.2 mg protein/ml) were incubated in the absence (control, spontaneous oxidation) or in the presence of HNE (1.1 and 2.2 nmoles/mg protein) in a metabolic shaker at 37 °C up to 1 h. In a parallel set of experiments, both control and HNE treated samples were preincubated for 5 min with the SH-alkylating agent NEM (1 mM final concentration). At fixed times (0, 30 and 60 min), 0.2 ml aliquots of each sample were spiked with the IS, BHT (0.1%, w/v) to stop lipid peroxidation, and then deproteinized and processed as described. Supernatants were directly analyzed by LC–MS/MS for HNE-peptide adducts detection. Additional 2 ml aliquots of the homogenates were incubated at 37 °C for 90 min in the presence of 20 mM AAPH to induce lipid peroxidation, and the time-course of Michael adducts formation monitored at 30 min intervals. The time-course of lipid peroxidation in control and in AAPH-treated samples was evaluated as TBARS (thiobarbituric acid-reactive substances) as previously described [13], using 0.5 ml of tissue homogenate.

3. Results and discussion

3.1. Method development

In previous studies [14] a sensitive, selective, specific and rapid liquid chromatographic–electrospray ionization tandem mass spectrometric (IT-MS) assay was developed and validated for the simultaneous determination of HD, carnosine, homocarnosine and anserine in biological matrices, in order to establish their plasma/tissue distribution. The chromatographic conditions, based on gradient elution with HFBA as ion pairing, was found to be suited not only for their quantitation, but also for the simultaneous detection of GSH and of the corresponding HNE-Michael adducts (Fig. 1) [7,8]. The water/acetonitrile/HCOOH gradient elution, typically used for peptide analysis, was not suited, since HD co-elute near the void volume, without improvement of the ionization efficiency for the HNE-HD adducts (data not shown). Hence the chromatographic conditions were maintained, while to increase sensitivity and reproducibility, the ion trap was replaced by a triple quadrupole system. H-Tyr-His-OH was maintained as internal standard for quantitative analysis because no isotopic derivatives of HNE adducts are commercially available; in addition, is it not present in tissues as endogenous peptide, it easily forms positive ions by ESI ionization, has a good recovery [14] and, as below reported, it is stable in our operative conditions. Hence as a first step we reinvestigated the CID patterns of the $[M + H]^+$ ions relative to the HNE adducts, to determine the optimal fragmentation reactions for MRM analysis, in terms of higher abundance and stability of at least two diagnostic product ions. Fig. 2 shows the CID spectra of CAR-HNE (a) and ANS-HNE (b) obtained by collision of the corresponding $[M + H]^+$ at *m*/*z* 383 and 397 (infusion experiments) at different collision energies. CAR-HNE at low collision energy shows only the ion at *m*/*z* 366 $[M + H–NH_3]^+$, as previously obtained with the IT-MS system [14], while the typical immonium ion of HNE-modified histidine residues [15,16] at *m*/*z* 266 reaches only 10% of relative abundance. By increasing collision energy up to 20 eV the ion at *m*/*z* 266 reaches almost 40% and concomitantly the product ion at *m*/*z* 110 (Hys immonium ion), due to a retro-Michael reaction from the ion at *m*/*z* 266 becomes evident. Optimization for these two diagnostic ions (relative abundances 100 and 95% respectively) was obtained at 35 eV collision energy.

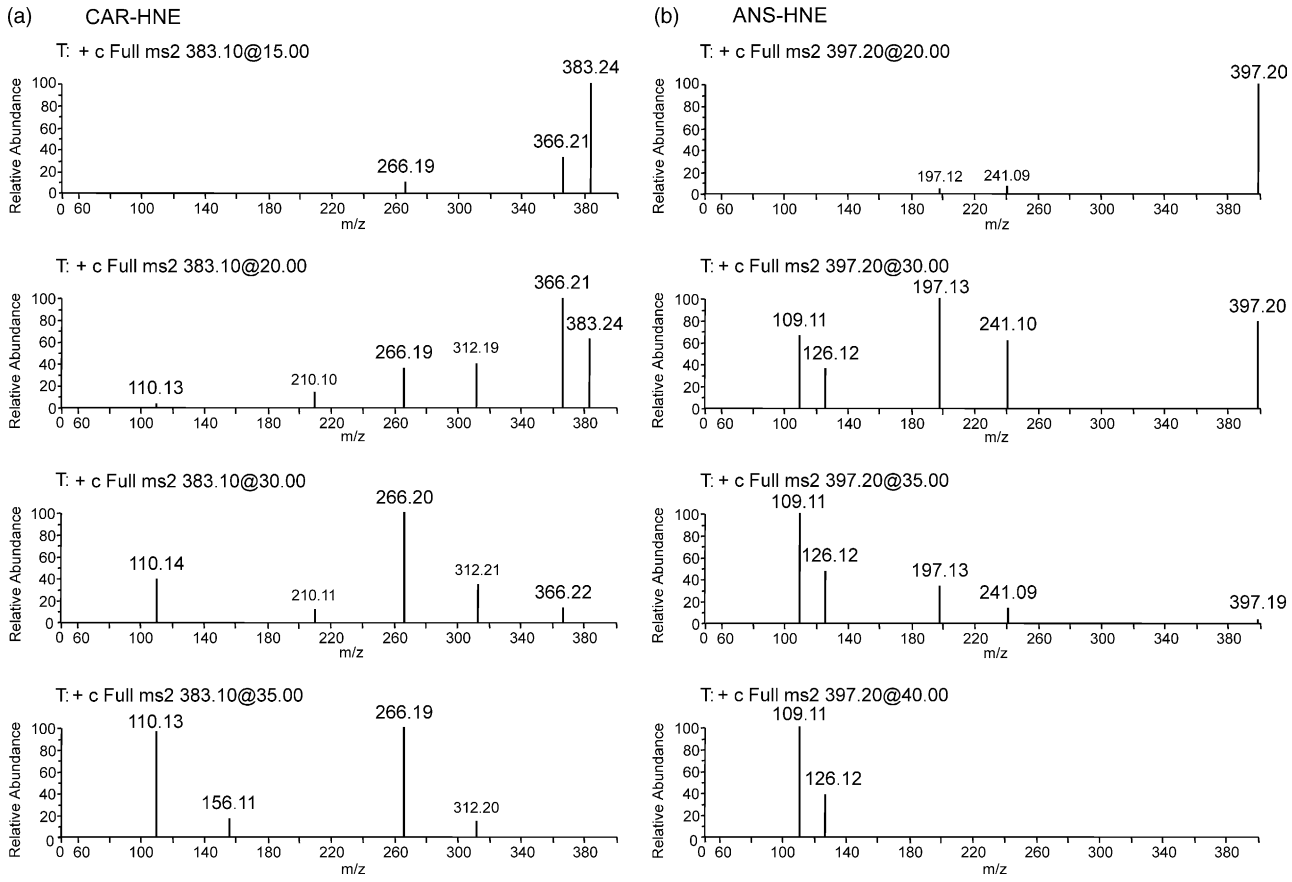

Fig. 2. ESI-MS2 spectra (positive-ion mode) of CAR-HNE (a) and ANS-HNE (b) recorded by colliding the $[M+H]^+$ at *m/z* 383 and 397 at increasing collision energies (infusion experiments).

Conversely, ANS-HNE at the highest collision energy (40 eV) shows as abundant product ions only those at *m/z* 126 and 109, attributable, as previously reported [14], to $[y+H{-}CO_2]^+$ and the corresponding $[y+H{-}CO_2{-}NH_3]^+$; no immonium ion at *m/z* 280, neither the retro-Michael fragment product $[M+H{-}HNE]^+$ at *m/z* 241, neither the corresponding product ion at *m/z* 197 due to sequential loss of CO_2 were present. The immonium ion was not detectable even lowering the collision energy to 20 eV, while the fragments at *m/z* 241 and 197 were prominent at 30 eV collision energy, to drastically decay at 35–40 eV. The same approach was applied to GS-HNE and IS: Table 1 shows the CID data obtained by colliding the corresponding $[M+H]^+$ at *m/z* 464 and 319 (optimized collision energies). The fragmentation pattern of GS-HNE, even at lower energies (data not shown), is dominated by the typical retro Michael reaction, with the ion at *m/z* 308, due to the neutral loss of 156 Da (HNE moiety), and minor fragments are at *m/z* 446 $[M+H{-}H_2O]^+$ and at *m/z* 179 (*y*2 ion). For the IS, the main product ions were at *m/z* 156 (the typical *y*), at *m/z* 301 $[M+H{-}H_2O]^+$ and at *m/z* 110 (Hys immonum ion). Table 1 also reports the optimized MRM transitions relative to GSH, CAR and ANS, obtained by colliding the $[M+H]^+$ at *m/z* 308, 227 and 241, respectively, used for detection of the endogenous peptides in the biological matrices.

On the basis of the MS^n fragmentation pathways, the following precursor-product ion combinations H-Tyr-His-OH (IS): *m/z* 319.2 → 156.5 + 301.6; GS-HNE: *m/z* 464.3 → 179.1 + 308.0; CAR-HNE: *m/z* 383.1 → 110.1 + 266.6; ANS-HNE: *m/z* 397.2 → 109.1 + 126.1 were used for Michael adducts quantitation.

Table 1
MRMs transitions for GS-HNE, internal standard, glutathione, carnosine and anserine

Analyte	MS	MS^2
GS-HNE	464.3 $[M+H]^+$	446.1 (20%) $[M+H{-}H_2O]^+$
		308.0 (100%) $[M+H{-}HNE]^+$
		179.1 (15%) (*y*2)
H-Tyr-His-OH	319.2 $[M+H]^+$	301.6 (40%) $[M+H{-}H_2O]^+$
		156.5 (100%) (*y*)
		110.2 (50%) (His immonium ion)
GSH	308.1 $[M+H]^+$	179.1 (50%) (*y*2)
		162.1 (100%) (*y*2 $-NH_3$)
CAR	227.1 $[M+H]^+$	156.6 (44%) (*y*)
		110.1 (100%) (His immonium ion)
ANS	241.2 $[M+H]^+$	109.2 (95%) $[y-CO_2{-}NH_3]^+$
		95.2 (100%) $[y-CO_2{-}NH_3{-}CH_3]^+$

3.2. Method validation

The LC–MS/MS profile of a mixture of GSH, CAR, ANS and of the corresponding HNE Michael adducts (and IS) indicates that all compounds elute with a typical bell peak shape (and within 1 min) at the following R.T.: GSH 3.80 min; CAR 4.50 min; ANS 4.65 min; IS 8.04 min; the HNE adducts coelute at 9.90 ± 0.05 min (data not shown). Specificity was demonstrated by the absence of interfering peaks in the mass and time ranges for HNE adducts and IS in all blank samples prepared from the different skeletal muscles (*tibialis* and *vastus* from five animals; triplicate injection). As a representative example, Fig. 3a reports the MRMs traces relative to tissue homogenate from *vastus* muscle. The endogenous peptides GSH, CAR and ANS are well detectable at the expected

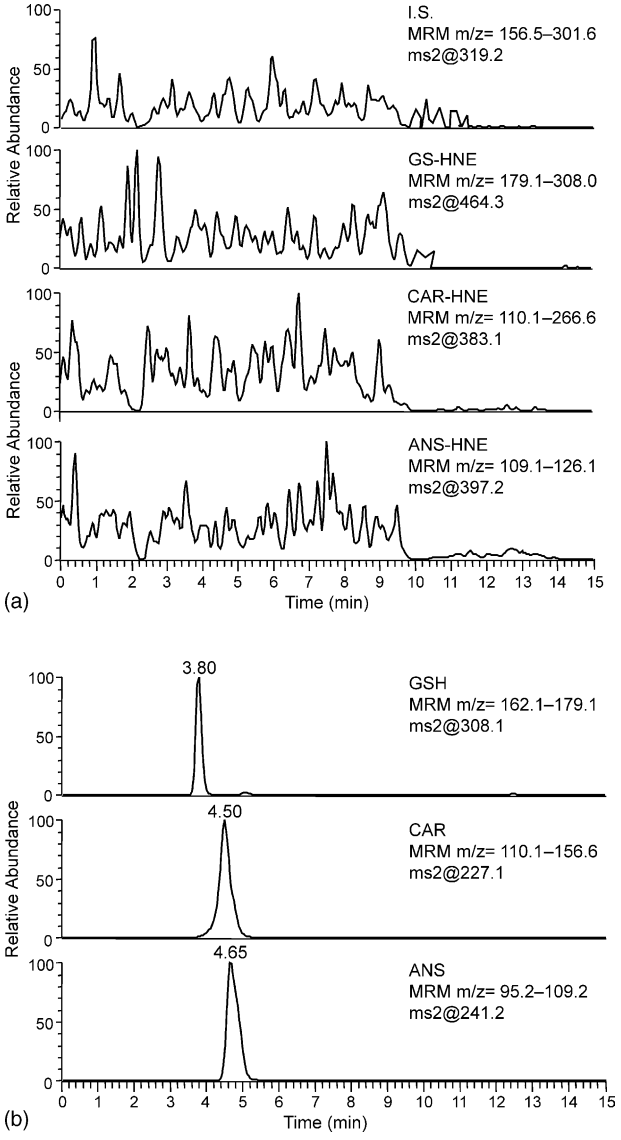

Fig. 3. LC–MS/MS profile of a blank tissue homogenate from *vastus* muscle. (a) MRMs traces relative to IS and peptides-HNE adducts and (b) MRMs traces relative to the endogenous peptides GSH, CAR and ANS.

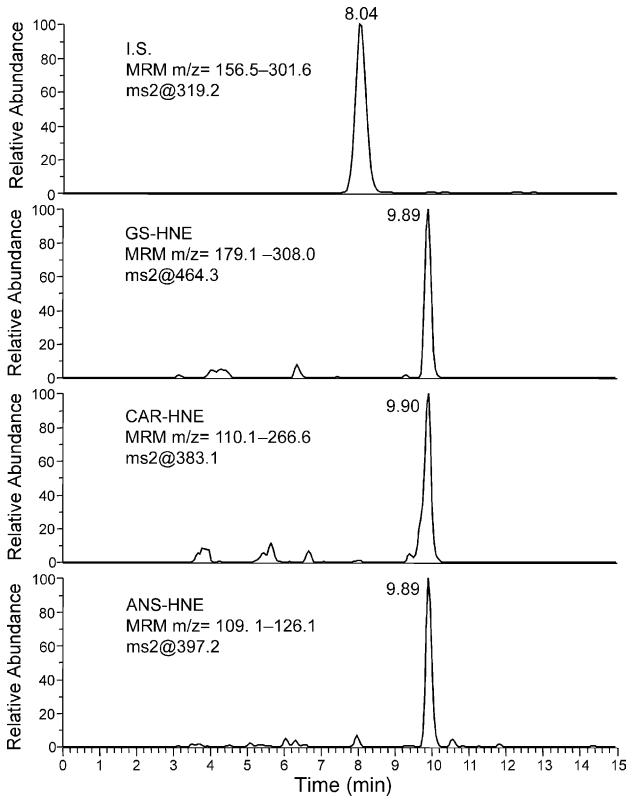

Fig. 4. LC–MS/MS profile of a blank tissue homogenate from *vastus* muscle spiked with IS (40 nmoles/g tissue) and the analytes at LLOQs (GS-HNE 1.5 nmoles/g; CAR-HNE and ANS-HNE 0.4 nmoles/g).

retention times in all the analyzed tissues (Fig. 3b), as previously reported working in IT-MS conditions [14].

Representative MRMs traces relative to the peptide-HNE adducts and IS (40 nmoles/g) obtained from *vastus* tissue homogenate spiked with LLOQ concentrations (1.5 nmoles/g GS-HNE; 0.4 nmoles/g CAR-HNE/ANS-HNE) are shown in Fig. 4. Similar results were obtained using *tibialis* muscle (data not shown). To demonstrate matrix-to-matrix reproducibility, five different blank samples from *vastus* and *tibialis* muscles were spiked with the analytes at the LLOQs. Precision and accuracy ranged from 5.38 to 9.2% (CV%) and from −16 to +12% (RE%), to indicate that there are no significant differences in the ionization efficiency between the two tissues.

Calibration curves for the analytes, constructed on different working days (*vastus* muscle), were used to determine GS-HNE and HD-HNE adducts concentrations in validation, QC, stability and study samples. The calibration curves were fit over the entire calibration ranges (1.5–90 nmoles/g GS-HNE; 0.4–40 nmoles/g HD-HNE), using a $1/x^2$ weighted quadratic fit and showed good linearity with correlation coefficients (r) greater than 0.998. The equations for the calibration lines were:

$y = 0.01870(\pm 0.00038)x + 0.04048(\pm 0.01757)$ GS-HNE;
$y = 0.11340(\pm 0.00138)x + 0.00813(\pm 0.00097)$ CAR-HNE;
$y = 0.13170(\pm 0.00233)x + 0.08294(\pm 0.00421)$ ANS-HNE.

Table 2
Intra- and inter-day accuracy and precision data for CAR-HNE, ANS-HNE and GS-HNE

Analyte	Nominal concentration (nmoles/g)	Mean measured concentration ± S.D. (nmoles/g)	Precision (CV%)	Accuracy (RE%)
Intra-day[a]				
CAR-HNE	0.4 (LLOQ)	0.39 ± 0.02	5.38	−2.50
	2	2.12 ± 0.09	4.15	6.00
	8	8.12 ± 0.16	1.97	1.55
	40	41.3 ± 0.50	1.21	3.25
ANS-HNE	0.4 (LLOQ)	0.45 ± 0.02	5.56	12.50
	2	2.14 ± 0.06	2.90	7.00
	8	8.14 ± 0.18	2.21	1.75
	40	40.90 ± 0.85	2.08	2.25
GS-HNE	1.5 (LLOQ)	1.26 ± 0.11	8.73	−16.00
	6	5.75 ± 0.35	6.09	−4.17
	30	30.91 ± 1.32	4.27	3.03
	90	92.01 ± 1.63	1.77	2.23
Inter-day[b]				
CAR-HNE	0.4 (LLOQ)	0.37 ± 0.03	8.38	−7.50
	2	2.11 ± 0.07	3.32	5.50
	8	8.17 ± 0.23	2.81	2.11
	40	39.34 ± 0.82	2.08	−1.65
ANS-HNE	0.4 (LLOQ)	0.46 ± 0.05	10.90	15.00
	2	2.13 ± 0.11	5.16	6.51
	8	8.18 ± 0.24	2.93	2.25
	40	39.87 ± 1.06	2.66	−0.32
GS-HNE	1.5 (LLOQ)	1.23 ± 0.13	10.56	−18.00
	6	5.70 ± 0.42	7.37	−5.00
	30	30.61 ± 1.87	6.10	2.03
	90	87.58 ± 4.50	5.14	−2.68

[a] Five replicates at each concentration level.
[b] Three runs, five replicates at each concentration level over a period of 3 days ($n = 15$).

The LOD (defined as $S/N > 3$) were 0.60 nmoles/g for GS-HNE and 0.15 nmoles/g for HD-HNE adducts (0.5 and 0.125 pmoles injected respectively) and the LLOQ were 1.5 nmoles/g for GS-HNE and 0.4 nmoles/g for HD-HNE adducts (1.25 and 0.33 pmoles injected respectively). The intra- and inter-assay precision and accuracy of the method were determined on QC samples by analysing five replicates at four concentration levels, and the data are reported in Table 2. The intra-day precision (CV%) was less than 6.10% (≤8.73% at the LLOQs) and accuracy ranged from −4.17 to +7.00% of nominal concentrations (within ± 16% at the LLOQs); the inter-day CV values were less than 7.38% (≤10.90% at the LLOQs) and accuracy was in the range −5.00 to +6.51% (within ± 18% at the LLOQs).

The extraction recovery was determined by comparing the peak area ratio of extracted tissue standards over the entire calibration range to those of post-extraction blank tissue homogenates spiked with the corresponding concentrations. The mean extraction recovery was satisfactory, being 97.0, 96.5 and 101.5% for GS-HNE, CAR-HNE and ANS-HNE, respectively.

The stability of the analytes was studied by considering the different steps of the overall procedure, and their determination was performed at the beginning and at the end of each storage period. Stability data, summarized in Table 3, indicated that the analytes were stable for at least the length of time under different conditions listed, all the values ranging from 95.8 to 105.5% of the initial value, except at the second freeze/thaw cycle, where adducts levels were decreased by 20–30%. Stability of stock solutions was also investigated. When stock solutions of HD-HNE in water were stored at a nominal temperature of 4 °C for 4 weeks, the analytes were stable (values between 97 and 101% of the initial value, data not shown).

To ensure the validity of HD-HNE adducts as biomarkers of oxidative stress, we also evaluated their stability in the biological matrix under phyisiological conditions (incubation at 37 °C for 2 h at the highest concentration level): while CAR-HNE was found to be highly stable (Table 3), GS-HNE and ANS-HNE levels were reduced by approximately 30% within the first 30 min and by 50% after 1 h. This probably reflects the metabolic conversion by oxidation/reduction of the aldehyde group, as demonstrated for GS-HNE in different tissues/organs, but never demonstrated in the skeletal muscle [6].

3.3. Application to HNE-supplemented and peroxidized rat skeletal muscles

The method was then applied to monitor the formation of HNE adducts in skeletal muscle homogenates (*vastus* and *tibialis*) spiked with physio-pathological HNE concentrations

Table 3
Stability of GS-HNE, CAR-HNE and ANS-HNE

Conditions	GS-HNE (nmoles/g)		CAR-HNE (nmoles/g)		ANS-HNE (nmoles/g)	
	30	90	20	40	20	40
1 h Short-term (4 °C)	98.7 ± 2.5	105.5 ± 3.6	102.7 ± 3.1	99.7 ± 4.8	101.6 ± 2.7	96.5 ± 3.4
24 h at 4 °C (AS)	102.7 ± 3.1	98.6 ± 2.6	102.4 ± 2.9	98.8 ± 4.8	101.6 ± 2.7	98.5 ± 3.4
4 Weeks at −20 °C	98.5 ± 2.7	103.9 ± 4.9	103.6 ± 3.5	99.3 ± 3.4	102.5 ± 1.7	97.7 ± 4.8
Freeze/thaw cycles						
First cycle	101.2 ± 2.6	99.2 ± 2.9	98.6 ± 3.7	104.7 ± 3.4	105.0 ± 2.8	95.8 ± 3.1
Second cycle	72.8 ± 3.1	79.5 ± 2.7	80.5 ± 4.2	76.5 ± 3.6	72.4 ± 1.9	69.5 ± 2.8

Incubation at 37 °C	GS-HNE 90 nmoles/g	CAR-HNE 40 nmoles/g	ANS-HNE 40 nmoles/g
30 min	70.7 ± 3.7	102.3 ± 2.1	72.7 ± 2.5
60 min	52.9 ± 3.4	99.7 ± 2.9	51.5 ± 3.2
90 min	38.4 ± 3.7	97.5 ± 2.8	43.4 ± 2.2
120 min	24.1 ± 2.8	91.6 ± 3.2	34.9 ± 3.1

Values (mean ± S.D. of three independent experiments) are reported as percent of the initial value.

levels, 125 and 250 nmoles/g (corresponding to 1.1 and 2.2 nmoles/mg protein) and in tissue homogenates left to spontaneous oxidation (incubation under aerobic conditions for 1 h). The same experiments were also performed in the presence of NEM, the well known alkylating agent for thiols, to mimick the abrupt decay in GSH pool, due to overproduction of free radicals, typical of an increased oxidative stress in muscle (exercise, aging). Fig. 5a reports the LC–MS/MS profiles obtained from *tibialis* muscle incubated for 60 min with the lowest HNE dose, where the typical MRMs peaks relative to GS-HNE, CAR-HNE and ANS-HNE adducts are easily detectable (although with different intensities) at the expected retention times (9.90 ± 0.05 min). As reasonable expectation, the signal intensity of the GS-HNE adduct drastically falls in

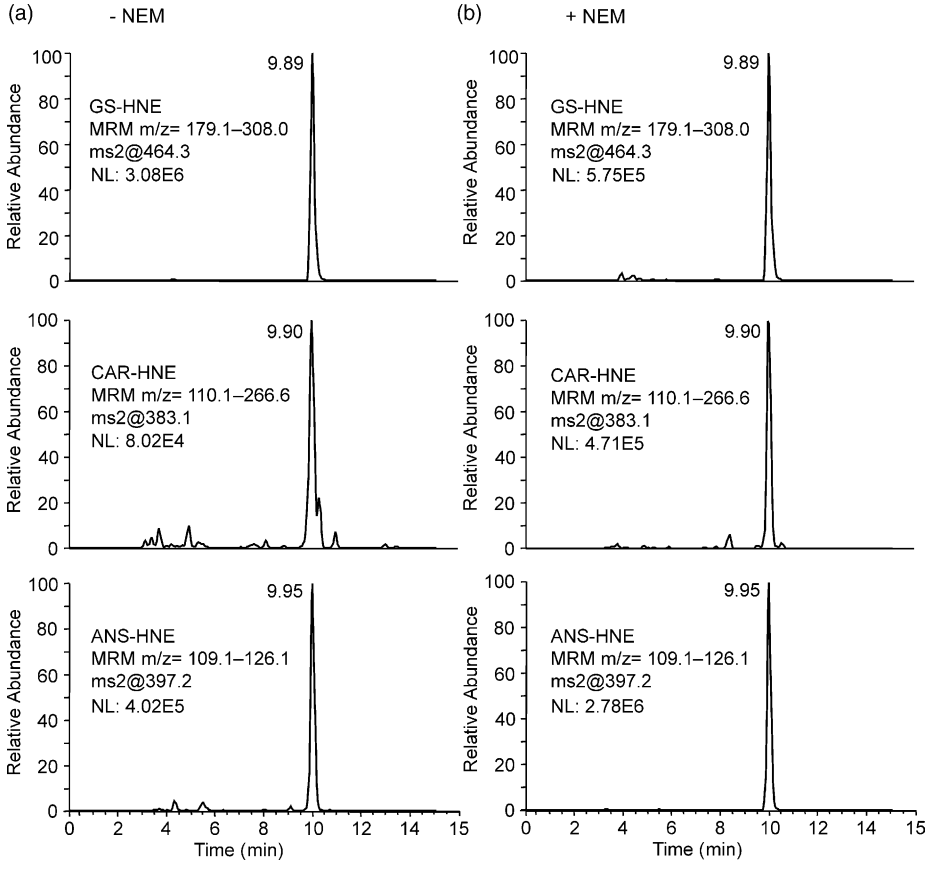

Fig. 5. LC–MS/MS profiles of tissue homogenate (*tibialis* muscle) incubated for 60 min with HNE (125 nmoles/g tissue) in the absence (a) and in the presence (b) of the thiol alkylating agent NEM (1 mM). At the end of the incubation time, 0.2 ml aliquots of the homogenate were spiked with the IS, deproteinized and processed as described in sample preparation.

Table 4
HNE adducts formation in spontaneously oxidized and HNE-spiked rat skeletal muscles

		Control spontaneous oxidation		HNE 125 nmoles/g		HNE 250 nmoles/g	
		−NEM	+NEM	−NEM	+NEM	−NEM	+NEM
Vastus muscle							
GS-HNE	30 min	BLQ	BLD	43.3 ± 1.95	4.38 ± 0.85	112.9* ± 7.90	5.31 ± 0.42
	60 min	BLD	BLD	31.2 ± 1.78	3.21 ± 0.15	64.2 ± 2.4	2.66 ± 0.18
CAR-HNE	30 min	BLQ	0.45 ± 0.08	BLQ	2.97 ± 0.41	0.56 ± 0.11	4.52 ± 0.26
	60 min	0.44 ± 0.09	0.58 ± 0.19	0.51 ± 0.04	3.15 ± 0.65	0.75 ± 0.08	4.38 ± 0.31
ANS-HNE	30 min	BLQ	BLQ	1.34 ± 0.18	18.74 ± 1.96	1.96 ± 0.61	28.59 ± 1.02
	60 min	BLD	BLD	0.87 ± 0.11	12.21 ± 1.48	1.15 ± 0.44	14.35 ± 0.93
Tibialis muscle							
GS-HNE	30 min	BLQ	BLD	29.10 ± 0.33	6.30 ± 0.58	52.12 ± 2.96	7.99 ± 0.61
	60 min	BLD	BLD	30.26 ± 1.58	5.96 ± 0.21	42.94 ± 2.57	4.36 ± 1.04
CAR-HNE	30 min	BLQ	BLQ	BLQ	0.52 ± 0.11	0.77 ± 0.08	2.18 ± 0.28
	60 min	BLQ	0.42 ± 0.04	0.47 ± 0.09	1.72 ± 0.66	0.73 ± 0.15	3.73 ± 0.77
ANS-HNE	30 min	BLQ	BLQ	0.86 ± 0.31	2.82 ± 0.41	4.63 ± 0.95	13.85 ± 1.21
	60 min	BLD	BLD	1.02 ± 0.15	6.98 ± 1.02	2.87 ± 0.21	15.83 ± 1.76

Values for HNE adducts (mean ± S.D. of three independent experiments; duplicate injection) are reported as nmoles/g wet tissue. BLQ: below the limits of quantitation; BLD: below the limits of detection.
* Determined on 1:2 diluted samples.

the corresponding sample pretreated with NEM, while those relative to HNE adducted HD-containing peptides are significantly increased (Fig. 5a). Table 4 summarizes the quantitative data relative to the entire set of experiments (those relative to the incubation time $t = 0$ are not reported, because preformed adducts were never detected in any biological matrix). The results indicate that: (a) HNE adducts formation in HNE-spiked samples is strictly dose-dependent; (b) the efficiency of *vastus* versus *tibialis* muscle in detoxyfing HNE (calculated as the sum of GS-HNE, CAR-HNE and ANS-HNE), is quite different: at 30 min approximately 46% of the added HNE (250 nmoles/g) is entrapped as peptide conjugates in *vastus* and 23% in *tibialis* (115.42 versus 57.52 nmoles/g HNE conjugated), where conjugation with GSH plays the key role; (c) in both skeletal muscles inhibition of the GSH-dependent pathway by NEM results in a significant elevation of both CAR-HNE and ANS-HNE levels (three-fold and more than eight-fold increase in *tibialis* and *vastus*, respectively); (d) in control samples (spontaneous oxidation), only CAR-HNE was formed and in low amount (GS-HNE and ANS-HNE were detectable at first 30 min, but below the limit of quantitation), to indicate an extremely low rate of lipid peroxidation. This was confirmed by the negative reaction in the TBARS assay, taking into account the sensitivity of the colorimetric test (1.5 nmoles/g) (data not shown).

Formation of HNE adducts was also evaluated in tissue homogenates (*vastus* and *tibialis* muscles) exposed to the radical initiator AAPH, an azo derivative which, generating peroxyl radicals at a constant rate, initiates and propagates lipid peroxidation. As shown in Fig. 6, at both the observation times and in both skeletal muscles, only CAR-HNE adduct was detectable, whose concentrations (0.65 and 1.35 nmoles/g at 30 and 60 min incubation in *vastus*; 0.48 and 0.72 nmoles/g in *tibialis*) time-dependently increase, in parallel to the increase of lipid peroxidation (TBARS assay). GS-HNE and ANS-HNE signals were always below the limit of detection: this might be due in part to a reduced availability of GSH, involved to counteract the peroxidation process (as confirmed by the time-dependent reduction in the GSH/IS peak area ratios, approximately 50 and 90% at 30 and 60 min), but also to their rapid decay in the biological matrix (see stability data). Moreover, although Cys is the most reactive residue toward

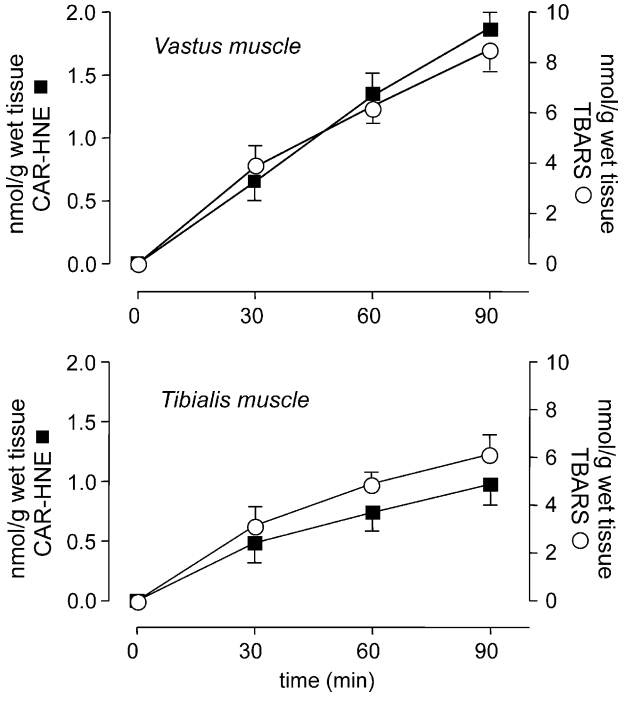

Fig. 6. Time-course of CAR-HNE and TBARS formation in rat skeletal muscles exposed to the radical initiator AAPH (20 mM) to induce lipid peroxidation. Values are the mean ± S.D. of three independent experiments (duplicate injection).

HNE if compared to His, the thiol adduct has been postulated to be less stable than His conjugates in biological matrices [17], due to a typical retro-Michael reaction. If this decay is due to metabolic conversion, it remains to be established.

4. Conclusions

The LC–MS/MS method here described, which allows the simultaneous detection in biological matrices of HNE conjugates, as GSH and HD Michael adducts, offers a new strategy in detecting and profiling the early markers of oxidative stress in excitable tissues. It requires minimal sample manipulation, due to a very simple deproteinization step without further purification, it is fast (total analysis time 30 min, including tissue processing and LC–MS analysis), sensitive and reliable.

An analytical method specifically designed to profile the levels of HNE adducts in biological matrices is of maximal utility from a biological and toxicological point of view, not only to elucidate the detoxification role of GSH and HD in other tissue/districts, but in view of the fact that such modified peptides would serve as early and sensitive biomarkers of oxidative damage, generally assessed in skeletal muscle by the poorly specific TBARS assay. To reach this goal, where detection limits are of paramount importance since the very low amounts of adducted peptide formed in biological samples, even more sensitive techniques are required, and the method here proposed fulfils these requirements. It is important to stress that conjugated adducts formation in skeletal muscles has been demonstrated first working with low HNE levels, strictly in the range of physio-pathological concentrations (HNE can reach relative large amounts in biological tissues, 5–10 μM at steady state concentration within membranes) [18]. The results confirm that GSH, due to the well known order of reactivity of the nucleophilic amino acids towards HNE Cys≫His>Lys [19], stems as the first line of defense against cytotoxic HNE also in skeletal muscle. Anyway, the GS-HNE adduct is a poorly reliable marker of oxidative stress: it is an intermediate and not an end product, since it can undergo metabolic conversion (reduction/oxidation of the aldehyde group), as demonstrated in many other tissues.

Moreover, our findings indicate that the histidine-dependent detoxification pathway becomes relevant when GSH levels are significantly reduced, suggesting a cooperative interaction between thiol and histidine-containing dipeptides, and above all highlight CAR-HNE as an early, specific and stable marker of oxidative stress. This taking into account that a suitable marker of oxidative damage must be (a) present in sufficiently high concentration in accessible tissues and fluids to enable collection and quantification; (b) sufficiently stable (no further degradation or generation of additional oxidation products when handled or stored). In this context, we have previously demonstrated for the first time to our knowledge that carnosine (and anserine) are present also in rat myocardium at significant levels (∼50 nmoles/g). This stems as another important finding at the light of the well documented carnosine's anti-ischemic activity, demonstrated in isolated rat heart and in vivo [20,21]. Future studies will be focused to demonstrate the suitability of this MS approach to detect/quantitate HD-HNE adduct formation in animal heart tissue under conditions that mimic pathological situations (myocardial post-ischemic conditions as a model of cardiovascular diseases), where HNE formation is massively involved.

Acknowledgement

Financial support from MIUR (Cofinanziamento Programma Nazionale 2004) is gratefully acknowledged.

References

[1] E.R. Stadtman, Ann. NY Acad. Sci. 928 (2001) 22.
[2] H.L. Refsgaard, L. Tsai, E.R. Stadtman, Proc. Natl. Acad. Sci. USA 97 (2000) 611.
[3] H. Esterbauer, R.J. Schaur, H. Zollner, Free Radic. Biol. Med. 11 (1991) 81.
[4] W. Siems, T. Grune, Mol. Aspects Med. 24 (2003) 167.
[5] J. Alary, F. Gueraud, J.P. Cravedi, Mol. Aspects Med. 24 (2003) 177.
[6] M. Carini, G. Aldini, R. Maffei Facino, Mass Spectrom. Rev. 23 (2004) 281.
[7] G. Aldini, M. Carini, G. Beretta, S. Bradamante, R. Maffei Facino, Biochem. Biophys. Res. Commun. 298 (2002) 699.
[8] G. Aldini, P. Granata, M. Carini, J. Mass Spectrom. 37 (2002) 1219.
[9] M. Carini, G. Aldini, G. Beretta, E. Arlandini, R. Maffei Facino, J. Mass Spectrom. 38 (2003) 996.
[10] G. Aldini, P. Granata, M. Orioli, E. Santaniello, M. Carini, J. Mass Spectrom. 38 (2003) 1160.
[11] M.A. Markwell, S.M. Haas, N.E. Tolbert, L.L. Bieber, Methods Enzymol. 72 (1981) 296.
[12] V.P. Shah, K.K. Midha, J.W.A. Findlay, et al., Pharm. Res. 17 (2000) 1551, Guidance for Industry, Bioanalytical Method Validation, U.S. Department of Health and Human Services, Food and Drug Administration, May 2001.
[13] M. Carini, G. Aldini, E. Bombardelli, P. Morazzoni, R. Maffei Facino, Life Sci. 67 (2000) 1719.
[14] G. Aldini, M. Orioli, M. Carini, R. Maffei Facino, J. Mass Spectrom. 39 (2004) 1417.
[15] M.S. Bolgar, S.J. Gaskell, Anal. Chem. 68 (1996) 2325.
[16] F. Fenaille, P.A. Guy, J.C. Tabet, J. Am. Soc. Mass. Spectrom. 14 (2003) 215.
[17] K. Uchida, Prog. Lipid Res. 42 (2003) 318.
[18] G. Poli, M.U. Dianzani, K.H. Cheeseman, T.F. Slater, J. Lang, H. Esterbauer, Biochem. J. 227 (1985) 629.
[19] J.A. Doorn, D.R. Petersen, Chem. Biol. Interact. 143–144 (2003) 93.
[20] J.W. Lee, H. Miyawaki, E.V. Bobst, J.D. Hester, M. Ashraf, A.M. Bobst, Mol. Cell Cardiol. 31 (1999) 113.
[21] S.L. Stvolinsky, D. Dobrota, Biochemistry (Mosc) 65 (2000) 849.